Title

Phosphorylation and protonation of neighboring MiRP2 sites: function and pathophysiology of MiRP2-Kv3.4 potassium channels in periodic paralysis.

Journal

FASEB journal : official publication of the Federation of American Societies for Experimental Biology, 20(2)

ISSN

0892-6638

Authors

Abbott, Geoffrey W
Butler, Margaret H
Goldstein, Steve AN

Publication Date

2006-02-01

DOI

10.1096/fj.05-5070com

Phosphorylation and protonation of neighboring MiRP2 sites: function and pathophysiology of MiRP2-Kv3.4 potassium channels in periodic paralysis

Geoffrey W. Abbott,[*] Margaret H. Butler,[†] and Steve A. N. Goldstein[†,1]

*Greenberg Division of Cardiology, Department of Medicine and Department of Pharmacology, Cornell University, Weill Medical College, New York, New York, USA; and [†]Department of Pediatrics and The Institute of Molecular Pediatric Sciences, University of Chicago, Pritzker School of Medicine, Chicago, Illinois, USA

ABSTRACT

MinK-related peptide 2 (MiRP2) and Kv3.4 subunits assemble in skeletal muscle to create subthreshold, voltage-gated potassium channels. MiRP2 acts on Kv3.4 to shift the voltage dependence of activation, speed recovery from inactivation, suppress cumulative inactivation and increase unitary conductance. We previously found an R83H missense mutation in MiRP2 that segregated with periodic paralysis in two families and diminished the effects of MiRP2 on Kv3.4. Here we show that MiRP2 has a single, functional PKC phosphorylation site at serine 82 and that normal MiRP2-Kv3.4 function requires phosphorylation of the site. The R83H variant does not prevent PKC phosphorylation of neighboring S82; rather, the change shifts the voltage dependence of activation and endows MiRP2-Kv3.4 channels with sensitivity to changes in intracellular pH across the physiological range. Thus, current passed by single R83H channels decreases as internal pH is lowered (pK_a ~7.3, consistent with histidine protonation) whereas wild-type channels are largely insensitive. These findings identify a key regulatory domain in MiRP2 and suggest a mechanistic link between acidosis and episodes of periodic paralysis.—Abbott, G. W., Butler, M. H., Goldstein, S. A. N. Phosphorylation and protonation of neighboring MiRP2 sites: function and pathophysiology of MiRP2-Kv3.4 potassium channels in periodic paralysis. FASEB J. 20, 293–301 (2006)

Key Words: KCNE3 · periodic paralysis · MiRP2 · Kv3.4

Genes in the KCNE family encode single transmembrane (TM) domain peptides that do not function alone but coassemble with pore-forming potassium channel cx-subunits to form heteromeric complexes with the unique attributes of native potassium currents (1, 2). Thus, MinK (KCNE1) associates with KCNQ1 to form a complex whose attributes closely resemble the cardiac current IKs (3, 4); MinK-related peptide 1 (MiRP1, encoded by KCNE2) assembles with HERG to pass currents like cardiac I_{Kr} (5) and MiRP2 (KCNE3), the subject of the present study, associates with Kv3.4 to form a skeletal muscle potassium channel that activates at subthreshold membrane potentials (6). The necessity for KCNE peptides in native ion channels to achieve normal function is made apparent by their requirement to recapitulate the characteristics of native currents in heterologous expression studies and by genetic and biophysical evidence associating their alteration with human disease. Thus, missense mutations in KCNE1 and KCNE2 yield abnormal MiRPs that alter function and are associated with inherited and acquired long QT syndrome (LQTS), a cardiac arrhythmia that predisposes to sudden death (5, 7–11); KCNE3 is associated with periodic paralysis (PP) (6), a genetically and phenotypically mixed group of skeletal muscle disorders, characterized by episodic attacks of weakness or paralysis (12, 13).

Disease-associated KCNE mutations identified to date reduce ability of channels to perform their normal role in repolarization due to diminished single channel conductance, a positive shift in the voltage dependence of activation, speeded deactivation, or a combination of these effects (6, 8, 14, 15). Some mutations are revealed clinically in response to a secondary, environmental stimulus. Thus, KCNE mutants associated with drug-induced arrhythmia include those with normal sensitivity to drug blockade (5, 16) and

[1] Correspondence: Department of Pediatrics and The Institute of Molecular Pediatric Sciences, University of Chicago, Pritzker School of Medicine, 5721 S. Maryland Ave., MC8000 (K160), Chicago, IL 60637, USA. E-mail: sangoldstein@uchicago.edu

doi: 10.1096/fj.05-5070com

others with increased drug sensitivity (5). A common polymorphism associated with drug-induced arrhythmia manifests normal channel function that is altered only on drug exposure due to increased sensitivity to block (8). Analogously, a missense variant of the cardiac voltage-gated sodium channel that is common in African Americans, and linked with arrhythmia in aging adults (17) as well as sudden infant death syndrome, yields a channel that operates normally at baseline but shows abnormal gain-in-function with lowered intracellular pH (18).

Here, we describe the influence of altered intracellular environment on normal and dysregulated function of MiRP2-Kv3.4 channels. We find that phosphorylation of serine 82 of MiRP2 (MiRP2-S82^{P}) is required for MiRP2 to produce the normal shift in voltage-dependent activation of Kv3.4 observed in vivo. The mutation of neighboring arginine 83 to histidine (MiRP2-R83H), associated with periodic paralysis, is found to mimic the effect of S82 dephosphorylation even though the change does not prevent phosphorylation of S82. Finally, the R83H variant confers sensitivity to lowered pH, offering a molecular rationale for the onset of periodic paralysis during activities that produce intracellular acidosis.

MATERIALS AND METHODS

Molecular biology

MiRP2 mutations were produced by pfu-based mutagenesis (QuickChange Kit; Stratagene, La Jolla, CA, USA) and confirmed by DNA sequencing. Human MiRP2 (acc no. AF076531) was cloned (5) and rat Kv3.4 (acc no. Q63734) was generously provided by B. Fakler (Tubingen). Genes were subcloned into pCINeo (Promega, Madison, WI, USA) for mammalian cell expression. A hemaglutinin (HA) epitope (sequence YPYDVPDYA) was inserted in the N terminus of MiRP2 to facilitate detection with anti-HA antibodies.

Biochemistry

COS-7 cells were cotransfected with Kv3.4 and HA-tagged wild-type or mutant MiRP2 constructs. Cells were harvested 48 h after transfection, solubilized at 4°C for 1 h in 200 mM KCl, 1% NP-40, 1% Triton X-100, 1% CHAPS, 0.1% SDS, 20 mM HEPES (pH 7.4) with protease inhibitors (Compete-EDTA free tablets; Roche, Basel, Switzerland). Lysates were cleared by centrifugation at 16,000 x g for 10 min at 4°C, then passed through Sephadex G-25 to remove nucleotides into a solution of 200 mM KCl, 1% NP-40, 1% Triton X-100, 1% CHAPS, 20 mM HEPES (pH 7.4), and protease inhibitors. The following reagents were then added and the solution incubated at 30°C: 1 mM sodium orthovanadate, 100 nM calyculin A, 1 µ,M cyclosporin A, 5 mM MgCl2, 5 mM ATP. After 30 min, 10 mM EDTA was added to terminate any phosphorylation reaction and the samples were placed on ice. MiRP2 was immunoprecipitated using 5 µ,g rat anti-HA antibody (Boehringer, Ingelheim, Germany) and protein G Sepharose (Pierce, Rockford, IL, USA). Samples were separated by SDS-PAGE (15% gels), followed by Western blot and detection of subunits by chemiluminesence using rabbit anti-phosphoserine antibody (Abcam, Cambridge, UK) or rabbit anti-HA antibody (Sigma, St. Louis, MO, USA) and HRP-conjugated secondary antibody.

Electrophysiology

For electrophysiology, Chinese hamster ovary (CHO) cells were transfected using Superfect (Qiagen, Valencia, CA, USA) with vectors carrying the cDNA for GFP, wild-type, or variant MiRP2 and Kv3.4. Currents were recorded by patch-clamp in cell-attached or off-cell, inside-out mode, 1–2 days after transfection. Recordings were obtained using an Axopatch 200A Amplifier (Axon Instruments, Foster City, CA, USA), an IBM computer and CLAMPEX software (Axon Instruments). Data analysis was performed using CLAMPFIT, FETCHAN, PSTAT (Axon Instruments) and TAC software (Instrutech, Great Neck, NY, USA). All recordings were performed at room temperature. Curves were fit to a Boltzmann function: $1/\{1 + \exp[(V_{1/2}-V)/V_s]\}$, where $V_{1/2}$ is the half-maximal voltage of activation and V_s the slope factor.

Protocols

Holding voltage was – 80 mV unless otherwise stated. For quantification of the voltage dependence of activation, cells were held at – 80 mV and pulsed in 10 mV, 3 s steps between –100 and +90 mV with a 5 s interpulse interval. For quantification of unitary current amplitude, cells were held at – 40 mV for 5–20 min.

Ionic conditions

Pipette and bath solution for CHO cells in cell-attached mode was (in mM): 100 KCl, 0.7 MgCl2, 1 CaCl2 , 10 HEPES (pH 7.4). Where appropriate, 10 nM phorbol-12-myristate-13 acetate (PMA) was included in the bath solution to stimulate PKC or 0.1 μ,M bis-indoylmaleimide (BIS) was included in the bath solution to inhibit PKC. For off-cell, inside-out recordings, pipette and bath solution were (in mM): 100 KCl, 0.7 MgCl, 1 $CaCl_2$; with 10 mM buffering agent that varied depending on pH range: MES, pH 6 – 6.5; HEPES, pH 7– 8; PIPES, pH 8.5–9.

RESULTS

MiRP2-S82 is a phosphorylation site

When identified in patients with periodic paralysis, MiRP2-R83H was studied and found to significantly alter the gating of MiRP2-Kv3.4 channels (6, 15). Specifically, wild-type MiRP2 shifts the midpoint voltage dependence of activation ($V_{1/2act}$) of Kv3.4 channels to a subthreshold potential (~ – 40 mV) while channels with R83H-MiRP2 show a suprathreshold value, $V_{1/2act}$ ~ –10 mV (15). Here, we explore the basis for the effect of the R83H mutation. Sequence analysis of human MiRP2 reveals that serine 82, neighboring R83, is within a predicted consensus protein kinase C (PKC) phosphorylation and that the site is conserved across the 5 members of the KCNE gene family (Fig. 1). We sought, therefore, to test the hypothesis that mutation at R83 altered function via an influence on the neighboring S82 phosphorylation site.

To determine if MiRP2 S82 is phosphorylated by PKC, COS cells were transfected with Kv3.4 and HA-tagged MiRP2 variants, for analysis by Western blotting using anti-phosphoserine antibodies. Following cell lysis and immunoprecipitation of wild-type MiRP2 (WT) using anti-HA, Western blot using anti-HA antibodies gave the expected bands (6) corresponding to the masses for the mature, immature and the carbohydrate-free glycosylation forms (Fig. 1C, lane 1). Western blotting using the anti-phosphoserine antibody revealed the same bands carried phosphoserine (Fig. 1D, lane 1). The same phosphoserine-positive bands were observed for MiRP2-R83H (Fig. 1D, lane 2) but not with MiRP2 variants, S82A and S82D, which remove the serine subject to phosphorylation (Fig. 1D, lanes 3 and 4). The results indicate that MiRP2 S82 can be phosphorylated by PKC, that this is the only MiRP2 site subject to modification, and that the R83H mutation does not prevent S82 phosphorylation.

MiRP2-S82 phosphorylation is required for subthreshold activation

The functional consequences of MiRP2 phosphorylation were assessed using patch clamp electrophysiology. Wild-type MiRP2-Kv3.4 channels readily reveal the most prominent influence of MiRP2 under base-line conditions, to produce subthreshold activation, when studied in cell-attached patches with symmetrical potassium across the membrane; wild-type MiRP2- Kv3.4 channels show significant inward current compared to channels with Kv3.4 alone (Fig. 2A) (6). Compared to those with wild-type MiRP2, Kv3.4 channels with S82A-MiRP2, a variant that is not phosphorylated (Fig. 1D), exhibit much less inward current at negative potentials (Fig. 2A). This is particularly noticeable by comparison of traces at – 40 mV (Fig. 2B, C) and suggests MiRP2 must bear phosphate to exert its full influence. Consistent with this

conclusion, wild-type MiRP2-Kv3.4 channels expressed in cells treated with PMA to stimulate PKC activity show prominent inward currents at – 40 mV while cells treated with BIS to inhibit PKC show reduced inward currents (Fig. 2D). Moreover, if phosphorylation of S82 mediates the effect, as expected, neither PMA nor BIS influence the operation of MiRP2-S82A-Kv3.4 channels (Fig. 2E). Another argument for a role of phosphate on serine 82 in the effect of MiRP2 is recapitulation of the phosphorylated phenotype when a negative charge is permanently substituted at MiRP2 position 82; MiRP2-S82D-Kv3.4 channels show significant inward currents at – 40 mV (Fig. 2B, C) in a manner that is insensitive to both PMA and BIS exposure (not shown).

Quantification of these effects (Table 1) shows that wild-type MiRP2-Kv3.4 channels in untreated cells activate with a $V_{1/2act}$ of ~– 40 mV, as before (6). This value was relatively unaffected by application of PMA, but was shifted to ~–10 mV by BIS application. S82A channels showed a $V_{1/2\ act}$ of ~–10 mV regardless of PMA or BIS treatment. S82D MiRP2Kv3.4 channels behaved similarly to wild-type MiRP2-Kv3.4 channels, with a $V_{1/2\ act}$ of activation of ~– 40 mV. For comparison, Kv3.4 alone channels were also assessed, giving a $V_{1/2act}$ of +9 mV, again similar to previous observations (6). These results are consistent with wild-type channels being constitutively phosphorylated by PKC at S82 and thus active at subthreshold potentials, and why they are largely unaffected by PKC stimulation, but show altered activity when PKC is inhibited. When S82 is mutated to A, PKC can no longer regulate MiRP2 via S82 and thus S82A channels are unresponsive to both activators and inhibitors of PKC. Conversely, the S82D change is found to mimic the effect of S82 phosphorylation yielding subthreshold activation.

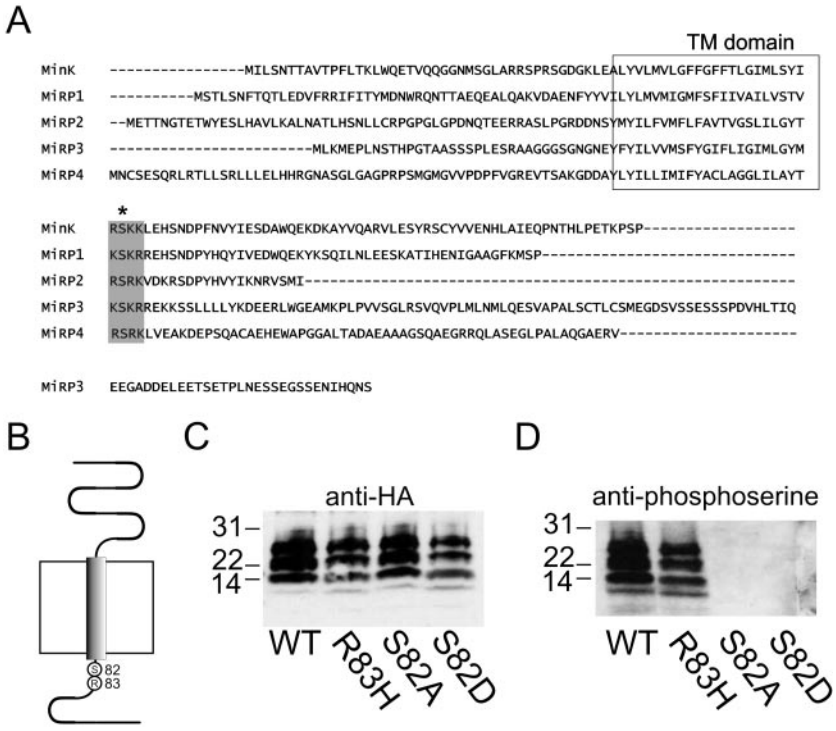

Figure 1. MiRPs contain a conserved consensus PKC phosphorylation site. A) Sequence alignment of MinK and MiRPs 1-4, performed with ClustalW. Predicted transmembrane (TM) domain is boxed. The consensus PKC phosphorylation site is highlighted in gray, with the predicted phosphorylated serine asterisked. B) Predicted topology of MiRP2 in the plasma membrane showing positioning of S82 and R83. C) Western blot of immunoprecipitates probed with rabbit anti-HA antibody show protein production of wild-type (WT) and MiRP2 variants. COS-7 cells were cotransfected with Kv3.4 and HA-tagged wild-type, S82A, S82D, or R83H MIRP2. Cells were lysed, treated with phosphatase inhibitors ATP and Mg2+, and then immunoprecipitated with rat anti-HA antibody, and analyzed by Western blot. Blots were visualized with HRP-labeled secondary antibodies and chemiluminescence. Migration of molecular weight markers is indicated by numbers on left of gels (kDa). D) Same samples as in panel C, probed with anti-phosphoserine antibody showing phosphorylation of MiRP2 proceeds for WT and R83H but not the S82A or D variants

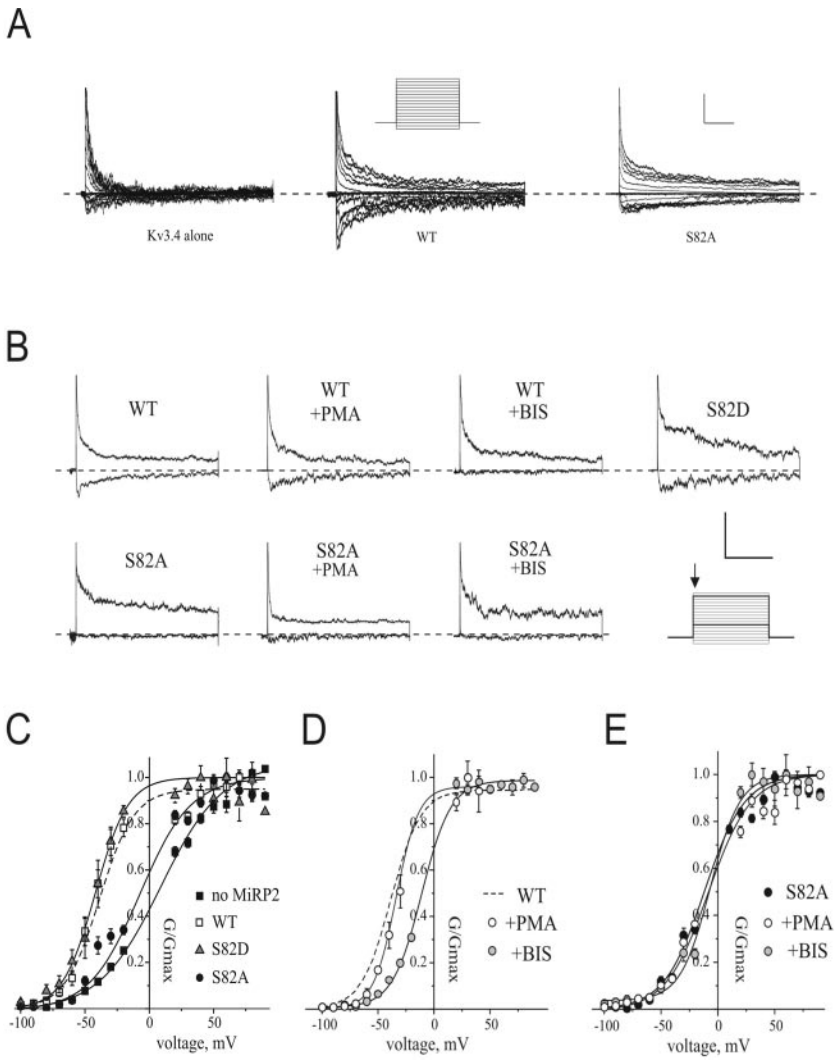

Figure 2. S82 phosphorylation is required for MiRP2 modulation of Kv3.4 gating. Studies of Kv3.4 channels alone or with wild-type (WT) or mutant MiRP2 performed in CHO cells in on-cell patch configuration with 100 mM KCl solution in bath and pipette using Protocol 1 (Materials and Methods). Data were collected at 5 kHz, digitally filtered at 1 kHz or 500 Hz. Exemplar cells expressing Kv3.4 alone, WT MiRP2-Kv3.4, and S82A-MiRP2-Kv3.4; current families recorded between –100 and 60 mV in patches with high channel density (inset, Protocol 1). Scale bars 30 pA (Kv3.4 alone) or 50 pA (with wild-type or S82A MiRP2) and 500 ms, dashed line represents zero current level. Exemplar traces recorded at +60 and – 40 mV from families recorded as in panel A, from channels formed by Kv3.4 and wild-type, S82A or S82D MiRP2, with or without application of 0.1 μ,M bisindoylmaleimide (BIS) or 10 nM phorbol-12-myristate-13 acetate (PMA) as indicated. C) Normalized peak current voltage relationship for Kv3.4 channels with no MiRP2 or with wild-type, S82A or S82D MiRP2; symbols as indicated. Error bars indicate se; n = 8 –9 patches per group. Curves were fit to a Boltzmann function. D) Normalized peak current voltage relationship for wild-type MiRP2- Kv3.4 channels without (dashed line) or with (solid lines) application of 0.1 μ,M bisindoyl-maleimide (BIS) or 10 nM phorbol-12-myristate-13 acetate (PMA); symbols as indicated. Error bars indicate se; n = 8 –11 patches per group. Curves were fit to a Boltzmann function. E) Normalized peak current voltage relationship for S82A MiRP2-Kv3.4 channels without or with application of 0.1 μ,M bisindoylmaleimide (BIS) or 10 nM phorbol-12-myristate-13 acetate (PMA); symbols as indicated. Error bars indicate se; n = 8 –14 patches per group. Curves were fit to a Boltz-mann function

R83H channels show abnormal activation, regardless of S82 phosphorylation state

R83H-MiRP2-Kv3.4 channels were shown to exhibit suprathreshold activation unlike wild-type MiRP2- Kv3.4 channels (6, 15). Here, we find that phosphorylation of S82 in wild-type MiRP2 is required to produce subthreshold activation (Fig. 2 and Table 1) and that R83H-MiRP2 is phosphorylated by PKC at

S82, arguing that failure to achieve subthreshold activation is not due to suppression of this event (Fig. 1C, D). Moreover, normal activation could not be restored in R83H channels by chemical or mutagenic addition of negative charge at S82. Thus, just as R83H-MiRP2 channels show suprathreshold activation ($V_{1/2act}$ ~–7 mV) (Fig. 3A, B), so, too, a double mutant carrying both the $S82^P$ mimic S82D and R83H (S82D, R83H-MiRP2) showed $V_{1/2act}$ ~–12mV (Fig. 3C). Furthermore, application of PMA to channels with R83H-MiRP2 had no significant effect on the voltage dependence of activation (Fig. 3A, C); application of BIS did shift $V_{1/2act}$ channels to –19 mV, ~10 mV more negative than the value for wild-type channels with BIS application.

TABLE 1. Voltage dependence of activation of channels formed by Kv3.4 alone or with variants of MiRP2a

Kv3.4 with:	Alone	Wild-type MiRP2			S82A-MiRP2		
stimulus	—	—	PMA	BIS	—	PMA	BIS
$V_{1/2act}$ (mV)	8.7 ± 1.5	−38.7 ± 1.6	−32.7 ± 1.7	−10.4 ± 0.7	−7.4 ± 1.1	−11.9 ± 0.6	−6.7 ± 1.4
slope (mV)	23.9 ± 1.0	13.4 ± 1.1	10.4 ± 1.0	13.5 ± 0.5	19.7 ± 0.7	17.7 ± 0.6	13.6 ± 0.9
n	9	11	8	9	8	14	8

[a] Phorbol-12-myristate-13 acetate (PMA) or bis-indolylmaleimide (BIS) was applied in some cases to stimulate or inhibit PKC activity, respectively. Values are shown ± SEM. $V_{1/2act}$, midpoint voltage dependence of activation; *n*, number of cells.

The R83H mutation confers sensitivity to inhibition by lowered intracellular pH

Lowered pH is a risk factor for some with periodic paralysis because attacks often occur with rest after exercise when serum and intracellular pH drop (19). Histidine can exist in both ionized and non-ionized forms at neutral pH (pKa ~7) and can mediate pH sensitivity of proteins, including ion channels (20, 21). The effects of altered intracellular pH (pH_i) on wild-type and R83H-MiRP2-Kv3.4 single channels were therefore examined at – 40 mV using inside-out patches from CHO cells; previously, we observed that channels with R83H-MiRP2 display lower unitary conductance than those with wild-type at physiological pH_i (15).

While wild-type MiRP2-Kv3.4 channels showed little variation in unitary current amplitude over the range pH_i 9.0 – 7.0, R83H-MiRP2-Kv3.4 complexes showed a steep decline across the physiological range (Fig. 4A). This effect was quantified by all-points histograms for each channel type at various pH_i levels and construction of proton-inhibition curves (Fig. 4B–D). The pH dependence of current suppression for wild-type MiRP2-Kv3.4 channels showed a half-maximal effect at ~ pH_i 6.0, compared to ~ pH_i 7.3 for R83H-MiRP2-Kv3.4 complexes (Fig. 4C, D). Dropping to pH_i 7.0 from 8.5 at – 40 mV reduced unitary current amplitude for channels with the R83H variant by 30% (to 1.20±0.21 pA from 1.70±0.14 pA) whereas wild-type channel amplitudes were reduced just 5% (to 1.90±0.18 pA from 2.0±0.1 pA). Kv3.4 channels with no MiRP2 showed no significant sensitivity over the pH_i range of 9.0 to 6.5 (Fig. 4C, D).

TABLE 1. (continued)

R83H-MiRP2			S82D-MiRP2	S82D, R83H-MiRP2
—	PMA	BIS	—	—
−7.4 ± 0.7	−1.3 ± 0.4	−18.9 ± 1.5	−42.0 ± 1.8	−11.7 ± 0.7
17.2 ± 0.6	14.9 ± 0.3	13.9 ± 1.3	12.8 ± 1.2	13.8 ± 0.5
14	5	7	8	8

DISCUSSION

MiRP2-Kv3.4 channel gating is tightly controlled by PKC phosphorylation

Wild-type MiRP2 shifts the potential for half-maximal activation of Kv3.4 channels ~ –50 mV (from $V_{1/2act}$~+9 mV to – 40 mV, Table 1; ref 6) to create subthreshold-activating channels; the disease-associated point change R83H suppresses this influence of MiRP2 yielding complexes with $V_{1/2act}$ ~–10 mV (Table 1; ref 15). To assess the basis for this effect of R83H, we first studied neighboring S82, showing it to be an operational site for PKC phosphorylation, the only such site in the peptide, and to mediate the major effect of wild-type MiRP2 on Kv3.4 channels, that is, the ~ –50 mV shift in $V_{1/2act}$. Mutation of MiRP2 S82 to A suppresses both phosphorylation of the peptide and its effects on Kv3.4 yielding $V_{1/2act}$ ~–7 mV. Further, an S82 to D mutation in MiRP2 allows it to serve like wild-type $S82^P$ MiRP2 yielding $V_{1/2act}$ ~– 42 mV.
A key role for PKC in Kv3.4 is already known; this pore-forming cx subunit has an amino-terminal inactivation domain of ~28 amino acids containing two PKC sites where phosphorylation acts to alter secondary structure and impair inactivation (22–25). Thus, MiRP2-Kv3.4 channels can be regulated by action of PKC on both MiRP2 and Kv3.4 subunits, with phosphorylation leading to increased current due to activation at more negative potentials and reduced inactivation.

A mechanistic link between lowered pH_i and attacks of periodic paralysis

To our surprise, the R83H change that suppressed the effects of S82 phosphorylation did not alter function by preventing phosphorylation of S82 or interfering with assembly of the MiRP2-Kv3.4 complexes (Fig. 1; ref 6). Moreover, the effect of R83H is dominant since subthreshold function is not restored to R83H-MiRP2- Kv3.4 channels by stimulation with PKC or MiRP2 double substitution (R83H, S82D-MiRP2). However, while wild-type channels were relatively insensitive to changes in intracellular pH across the physiological range, R83H-MiRP2-Kv3.4 channels showed a significant decrease in current with lowered pH_i. The most noticeable effect of the R83H mutation is the shift of ~–35 mV in activation voltage that decreases open probability at normal pH; lowering pH_i further exacerbates this loss in function that may precipitate a clinical event. Although an S82 to D change mimics the effect of phosphorylated MiRP2 on Kv3.4 and suggests a negative charge is necessary and sufficient at the site, charge similarity does not appear adequate to restore native function to channels with R83H MiRP2, since lowered pH is likely to protonate the mutant histidine but further reduces similarity to wild-type. This suggests R83 may participate in important protein-protein contacts, perhaps with residues from Kv3.4.

Attacks of hypokalemic familial PP often occur during rest after exercise (26, 27), as observed with one of our patients (6). While lowered serum potassium may be causative in these cases, another potential explanation is reduced pH_i. During the first 5–10 s of exercise, metabolic alkalosis occurs apparently due to intracellular phosphocreatine hydrolysis, H^+ efflux and H^+ movement into sarcoplasmic reticulum (28 –33). Additional exercise leads to lower plasma and skeletal myocyte pH as lactic acid is produced, VO_2 and local PCO_2 increase, and H^+ transport processes are reversed (28, 29, 31–33); acidosis facilitates oxygen dissociation from hemoglobin during exercise (31, 34). In mammalian skeletal muscle pH_i is reported to drop below 6.5 with exercise: 6.28 was recorded in canine gracilis muscle after 3 min of exercise (28); 6.5 was recorded in human gastrocnemius after 30 s of exercise (35); 6.4 was reported in human forearm after exercise to fatigue (36). Early in post-exercise recovery human muscle pH_i is reported to become still lower (35, 36). Thus, protonation of a substituted histidine in MiRP2 position 83 provides a possible link between exercise, acidosis, and the onset of paralysis. At baseline, channels with R83H MiRP2 pass less current than wild-type and as pH drops below 7.0 another ~1/3 of the current (assessed at – 40 mV) will be lost.

Although sustained weakness can occur in some individuals with age, attacks of paralysis are not permanent and often manifest with an environmental demand. This type of superimposition of genetic factors predisposing to risk with a secondary environmental challenge is analogous to the apparent mechanisms for some acquired cardiac arrhythmias where events occur due to diminished repolarization capacity at baseline, exacerbated by normal (8) or increased sensitivity to drug blockade (5). Particularly

relevant to this report is a missense variant in the cardiac voltage-gated sodium channel common in African Americans that operates normally at baseline but shows abnormal gain-in-function with lowered intracellular pH (18) and is linked to arrhythmia in aging adults (17) and sudden infant death syndrome (18).

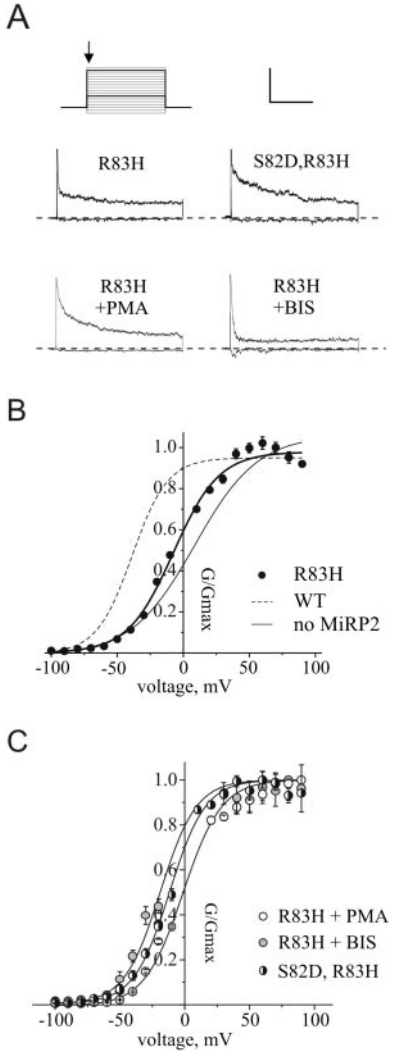

Figure 3. A negative charge at S82 does not restore subthreshold activation in R83H MiRP2-Kv3.4 channels. Studies of R83H or R83H, S82D MiRP2-Kv3.4 channels were performed in CHO cells in on-cell patch configuration with 100 mM KCl solution in bath and pipette using Protocol 1 (Materials and Methods). Data were collected at 5 kHz, digitally filtered at 1 kHz or 500 Hz. A) Exemplar traces recorded at +60 and – 40 mV from families recorded between –100 and 60 mV in patches with high channel density (inset, Protocol 1) from channels formed by Kv3.4 and R83H or R83H, S82D MiRP2, with or without application of 0.1 μ,M bisindoylmaleimide (BIS) or 10 nM phorbol-12-myristate-13 acetate (PMA) as indicated. B) Normalized peak current voltage relationship for channels formed with Kv3.4 and R83H-MiRP2 (filled circles) with curves for Kv3.4 with no MiRP2 (solid line) or wild-type MiRP2 (dashed line) shown for comparison. Error bars indicate se; n = 9 –14 patches per group. Curves were fit to a Boltzmann function. C) Normalized peak current voltage relationship for R83H-MiRP2-Kv3.4 channels with application of 0.1 μ,M bisindoylmaleimide (BIS) or 10 nM phorbol-12-myristate-13 acetate (PMA); or R83H, S82D MiRP2- Kv3.4 channels; symbols as indicated. Error bars indicate se; n = 5– 8 patches per group. Curves were fit to a Boltzmann function.

The sensitivity of R83H-MiRP2 channels to lowered pH_i is also a possible explanation for apparently paradoxical results of treatment of some patients with the carbonic anhydrase inhibitor acetazolamide. While acetazolamide often decreases the frequency of PP attacks by causing metabolic acidosis and preventing intracellular potassium shifts (37), the agent can precipitate events in some (38). Thus, maintaining a normal pH_i might prove more valuable in patients with R83H- MiRP2 than stabilizing intracellular potassium levels at the expense of pH. Acetazolamide slows the rate of recovery of normal

intracellular pH during rest after exercise and reduces the absolute pH reached during exercise and recovery (36). This draws comparisons to treatment of cardiac arrhythmia, where some anti-arrhythmic drugs are pro-arrhythmic due to blockade of cardiac delayed rectifier potassium channels, especially I_{Kr} (8).

R83H-MiRP2 and linkage to PP

Periodic paralysis is a genetically and phenotypically heterogeneous group of episodic skeletal muscle disorders characterized by prolonged episodic attacks of weakness or paralysis (12, 39). Given the overlap of symptoms, and as different forms of PP are associated with mutations in several skeletal muscle ion channel genes, a useful classification will be one based on genotyping (12, 40) both as a strategy to target optimal therapy and avoid complications like those described above for acetazolamide.

PP has been associated with mutations in the L-type calcium channel gene (CACNLA3) (41, 42), the voltage-gated sodium channel gene (SCN4A) (43– 47), and MiRP2 (KCNE3) (6). The related muscle disorder myotonia congenita is linked to mutations in a chloride channel gene (CLCN1) (48, 49). Andersen's syndrome, a disorder in which patients present with developmental defects, cardiac arrhythmia, and periodic paralysis, is caused by mutation of the inward rectifier potassium channel gene KCNJ7 (50). After the original report of association of KCNE3 mutation with PP (6), linkage of R83H-MiRP2 has been questioned based on observations of the genotype in 3 of 320 controls and a family with PP where it did not segregate with disease, although, that kindred had another mutation to explain the disease (51). We found the R83H variant in two small pedigrees in all individuals with PP and not in unaffected relatives, and did not observe the variant in 100 controls (6). This was suggestive for association with disease, but it was the functional effects of the amino acid change that made the case for linkage so strong (6). The possibility remains that R83H is predisposing for PP and must be present with some other genetic variant (such as a promoter variant that leads to a higher level of the R83H allele or changes the operation of some other protein); in that case, cosegregation in our kindreds could be because of linkage to the additional change or coincidence. The current report suggests that R83H-MiRP2 subunits might predispose to PP by creating channels that are sensitive to lowered intracellular pH, yielding a secondary challenge to normal muscle function from a common change in acid-base status in response to intense exercise. The data supporting the conclusion that R83H is a periodic paralysis gene are compelling: occurrence in patients from two affected families, presence of message and protein in the appropriate human tissue, interaction of MiRP2 with Kv3.4 in rat and mouse muscle, functional effects of assembly of the subunits, functional changes on expression of the mutation in muscle cells consistent with disease, and a mechanistic link between dysfunction of R83H-MiRP2-Kv3.4 channels and a known precipitating agent in some cases of PP, intracellular acidosis.

A KCNE domain critical to gating and conduction

The membrane-following region of MiRP2 contains a number of features highly conserved among KCNE peptides: a cluster of basic residues, a consensus protein kinase C (PKC) phosphorylation site, and a conserved aspartic acid (position 90 in MiRP2) (1). The basic residues are present in all five known KCNE peptides; the aspartic acid is conserved in MinK (D76), MiRP1 (D82), MiRP2 (D90) and MiRP4 (D92). In

MinK and MiRP2 a D-N mutation at this position causes reduced unitary conductance and altered gating; in MinK this mutation causes Romano-Ward and Jervell and Lange-Nielsen syndromes (manifesting cardiac arrhythmia without and with sensorineural deafness, respectively) (10, 14, 15). Mutation of nearby S74 to L in MinK also reduces current density and is associated with cardiac arrhythmia (10, 14).

Like R83 in MiRP2, MinK and MiRP1 contain lysine in the analogous site and mutant changes have similar effects. Thus, R83H-MiRP2, K69H-MinK, and K75H- MiRP1 have blunted effects compared with wild-type on cx-subunits in the resultant I_{Ks} and I_{Kr} channels (15). Further, R83H in MiRP2 affects not only complexes with Kv3.4 but the properties of MiRP2/KCNQ1 and MiRP2/HERG channels (15). While channel function is sensitive to changes in this conserved region, it should be noted that mutations do not

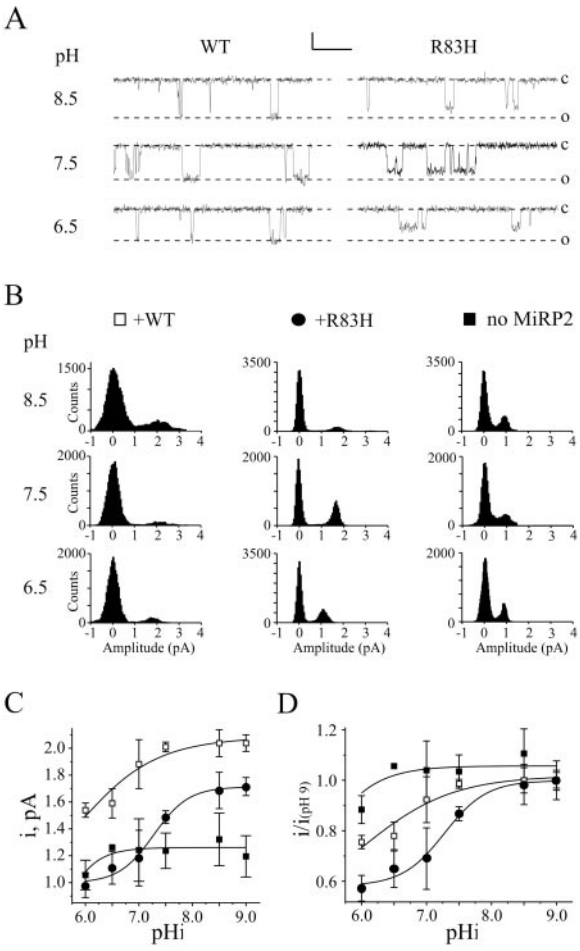

Figure 4. The R83H mutation in MiRP2 increases sensitivity to low pH of MiRP2/Kv3.4 channels. Studies of Kv3.4 with or without wild-type or R83H-MiRP2 single channel currents expressed in CHO cells were performed in inside-out patches with varying "internal" pH as indicated at – 40 mV with 100 mM KCl solution in the bath and pipette. Data were collected at 5 kHz, low-pass filtered at 500 Hz. A) Exemplar single channel current recordings from channels formed by Kv3.4 and wild-type (WT) or R83H-MiRP2, at pH 6.5, 7.5 and 8.5. Dashed lines indicate wild-type open state level ("o") and closed state ("c"). Scale bars indicate 1 pA and 100 ms. B) Representative all-points histograms from recordings at "intracellular" pH 6.5, 7.5 and 8.5, for single WT MiRP2-Kv3.4 (open squares) and R83H-MiRP2-Kv3.4 (filled circles) channels; histogram for homomeric Kv3.4 (filled squares) channels shown for comparison. C) Mean unitary current amplitudes at – 40 mV in a range of intracellular pH values between 6 and 9 for WT (open squares) and R83H (filled circles) MiRP2-Kv3.4 channels, or homomeric Kv3.4 channels (filled squares) calculated using all-points histograms as in panel B (n=3–5 patches per point), error bars indicate se. Curves were fit to the function: $y = [A_1\text{-}A_2 / \{1+(x/x_0)^p\}]+A_2$, where x = pH, x0 = the inhibition constant, and p = the Hill coefficient. WT MiRP2/Kv3.4 channels: A1 = 0.91 ± 0.15, A2 = 2.1 ± 0.08, x0 = 6.0 ± 1.7, P = 0.70 ± 0.25; R83H-MiRP2-Kv3.4 channels: A1 = 1.0 ± 0.06, A2 = 1.7 ± 0.04, x0 = 7.3 ± 0.11, P = 0.33 ± 0.1; homomeric Kv3.4 channels: A1 = 0.78 ± 0.28, A2 = 1.3 ± 0.05, x0 = 5.2 ± 59, P = 0.35 ± 2.5. D) Mean normalized unitary current amplitudes at – 40 mV in a range of intracellular pH values for WT (open squares) and R83H (filled circles) MiRP2-Kv3.4 channels, or homomeric Kv3.4 channels (filled squares) as in panel B; values normalized to unitary current amplitudes at pH 9.0. Curves were fit to the function: $y = [A_1\text{-}A_2 /\{1+(x/x_0)^p\}] + A_2$, where x is pH, x0 the inhibition constant and p the Hill coefficient. WT MiRP2-Kv3.4 channels: A1 = 0.53 ± 0.06, A2 = 1.0 ± 0.03, x0 = 6.2 ± 0.1, P = 0.62 ± 0.21; R83H-MiRP2-Kv3.4 channels: A1 = 0.58 ± 0.04, A2 = 1.0 ± 0.02, x0 = 7.3 ± 0.11, P = 0.34 ± 0.12; homomeric Kv3.4 channels: A1 = 0.26 ± 0.83, A2 = 1.1 ± 0.06, x0 = 5.2 ± 59.2, P = 0.44 ± 4.0

have effects in all MiRP-cx subunit complexes; R83H–MiRP2 does not disrupt function of complexes formed by MiRP2 and Kv2.1 or Kv3.1, perhaps because in these complexes MiRP2 alters the rate but not the voltage dependence of activation (52). Future studies addressing how this critical MiRP region interacts with pore-forming subunits should yield insight into normal function and mechanisms of inherited and

acquired human disease.

G.W.A. is supported by the NIH and the American Heart Association. S.A.N.G. is supported by the NIH and a Doris Duke Foundation Distinguished Clinical Scientist Award. We thank R. Goldstein for thoughtful discussions.

REFERENCES

1. Abbott, G. W., and Goldstein, S. A. (1998) A superfamily of small potassium channel subunits: form and function of the MinK-related peptides (MiRPs). *Q. Rev. Biophys*. 31, 357–398
2. McCrossan, Z. A., and Abbott, G. W. (2004) The MinK-Related Peptides. Neuropharmacology 47, 787– 821
3. Barhanin, J., Lesage, F., Guillemare, E., Fink, M., Lazdunski, M., and Romey, G. (1996) K(V)LQT1 and lsK (minK) proteins associate to form the I(Ks) cardiac potassium current. *Nature (London)* 384, 78–80
4. Sanguinetti, M. C., Curran, M. E., Zou, A., Shen, J., Spector, P. S., Atkinson, D. L., and Keating, M. T. (1996) Coassembly of K(V)LQT1 and minK (IsK) proteins to form cardiac I(Ks) potassium channel. *Nature (London)* 384, 80–83
5. Abbott, G. W., Sesti, F., Splawski, I., Buck, M. E., Lehmann, M. H., Timothy, K. W., Keating, M. T., and Goldstein, S. A. (1999) MiRP1 Forms IKr Potassium Channels with HERG and Is Associated with Cardiac Arrhythmia. *Cell* 97, 175–187
6. Abbott, G. W., Butler, M. H., Bendahhou, S., Dalakas, M. C., Ptacek, L. J., and Goldstein, S. A. (2001) MiRP2 forms potassium channels in skeletal muscle with Kv3.4 and is associated with periodic paralysis. *Cell* 104, 217–231
7. Isbrandt, D., Friederich, P., Solth, A., Haverkamp, W., Ebneth, A., Borggrefe, M., Funke, H., Sauter, K., Breithardt, G., Pongs, O., et al. (2002) Identification and functional characterization of a novel KCNE2 (MiRP1) mutation that alters HERG channel kinetics. *J. Mol. Med*. 80, 524 –532
8. Sesti, F., Abbott, G. W., Wei, J., Murray, K. T., Saksena, S., Schwartz, P. J., Priori, S. G., Roden, D. M., George, A. L., Jr., and Goldstein, S. A. (2000) A common polymorphism associated with antibiotic-induced cardiac arrhythmia. *Proc. Natl. Acad. Sci. USA* 97, 10613–10618
9. Splawski, I., Timothy, K. W., Vincent, G. M., Atkinson, D. L., and Keating, M. T. (1997) Molecular basis of the long-QT syndrome associated with deafness. *N. Engl. J. Med.* 336, 1562–1567
10. Splawski, I., Tristani-Firouzi, M., Lehmann, M. H., Sanguinetti, M. C., and Keating, M. T. (1997) Mutations in the hminK gene cause long QT syndrome and suppress IKs function. *Nat. Genet.* 17, 338 –340
11. Tyson, J., Tranebjaerg, L., Bellman, S., Wren, C., Taylor, J. F., Bathen, J., Aslaksen, B., Sorland, S. J., Lund, O., Malcolm, S., et al. (1997) IsK and KvLQT1: mutation in either of the two subunits of the slow component of the delayed rectifier potassium channel can cause Jervell and Lange-Nielsen syndrome. *Hum. Mol. Genet.* 6, 2179 –2185
12. Ptacek, L. (1998) The familial periodic paralyses and nondystrophic myotonias. *Am. J. Med.* 105, 58 –70
13. Ptacek, L. J. (1999) Channelopathies: ion channel disorders of muscle as a paradigm for paroxysmal disorders of the nervous system. Dig. Dis. Sci. 44, 94S–96S
14. Sesti, F., and Goldstein, S. A. (1998) Single-channel characteristics of wild-type IKs channels and channels formed with two minK mutants that cause long QT syndrome. *J. Gen. Physiol.* 112, 651–663
15. Abbott, G. W., and Goldstein, S. A. (2002) Disease-associated mutations in KCNE potassium channel subunits (MiRPs) reveal promiscuous disruption of multiple currents and conservation of mechanism. *FASEB J.* 16, 390 – 400
16. Park, K. H., Kwok, S. M., Sharon, C., Berga, R., and Sesti, F. (2003) N-glycosylation-dependent

block is a novel mechanism for drug-induced cardiac arrhythmia. *FASEB J.* 17, 2308 –2309
17. Splawski, I., Timothy, K. W., Tateyama, M., Clancy, C. E., Malhotra, A., Beggs, A. H., Cappuccio, F. P., Sagnella, G. A., Kass, R. S., and Keating, M. T. (2002) Variant of SCN5A sodium channel implicated in risk of cardiac arrhythmia. *Science* 297, 1333–1336
18. Plant, L. D., Bowers, P. N., Liu, Q., Morgan, T., Zhang, T., State, M. W., Chen, W., Kittles, R. A., and Goldstein, S. A. N. (2005) A common cardiac sodium channel variant associated with sudden infant death in African Americans, SCN5A-S1103Y. *J. Clin. Invest.* In press
19. Kuzmenkin, A., Muncan, V., Jurkat-Rott, K., Hang, C., Lerche, H., Lehmann-Horn, F., and Mitrovic, N. (2002) Enhanced inactivation and pH sensitivity of Na(+) channel mutations causing hypokalaemic periodic paralysis type II. *Brain* 125, 835– 843
20. Landau, E. M., Gavish, B., Nachshen, D. A., and Lotan, I. (1981) pH dependence of the acetylcholine receptor channel: a species variation. *J. Gen. Physiol.* 77, 647– 666
21. Lopes, C. M., Zilberberg, N., and Goldstein, S. A. (2001) Block of Kcnk3 by protons. Evidence that 2-P-domain potassium channel subunits function as homodimers. *J. Biol. Chem.* 276, 24449 – 24452
22. Schroter, K. H., Ruppersberg, J. P., Wunder, F., Rettig, J., Stocker, M., and Pongs, O. (1991) Cloning and functional expression of a TEA-sensitive A-type potassium channel from rat brain. *FEBS Lett.* 278, 211–216
23. Covarrubias, M., Wei, A., Salkoff, L., and Vyas, T. B. (1994) Elimination of rapid potassium channel inactivation by phosphorylation of the inactivation gate. *Neuron* 13, 1403–1412
24. Stephens, G. J., and Robertson, B. (1995) Inactivation of the cloned potassium channel mouse Kv1.1 by the human Kv3.4 “ball” peptide and its chemical modification. *J. Physiol. (London)* 484, 1–13
25. Antz, C., Bauer, T., Kalbacher, H., Frank, R., Covarrubias, M., Kalbitzer, H. R., Ruppersberg, J. P., Baukrowitz, T., and Fakler, B. (1999) Control of K+ channel gating by protein phosphorylation: structural switches of the inactivation gate. *Nat. Struct. Biol.* 6, 146 –150
26. Gamper, G., Stulnig, T., and Weissel, M. (1998) Thyrotoxic hypokalemic periodic paralysis in a male Kurd. *Acta Med. Austriaca* 25, 106 –108
27. Tengan, C. H., De Oliveira, A. S., and Gabbai, A. A. (1994) Periodic paralysis. Clinical analysis in 20 patients. *Arq. Neuropsiquiatr.* 52, 501–509
28. Connett, R. J. (1987) Glycolytic regulation during an aerobic rest-to-work transition in dog gracilis muscle. *J. Appl. Physiol.* 63, 2366 –2374
29. Connett, R. J. (1987) Cytosolic pH during a rest-to-work transition in red muscle: application of enzyme equilibria. *J. Appl. Physiol.* 63, 2360 –2365
30. Adams, G. R., Foley, J. M., and Meyer, R. A. (1990) Muscle buffer capacity estimated from pH changes during rest-to-work transitions. *J. Appl. Physiol.* 69, 968 –972
31. Barstow, T. J., Buchthal, S., Zanconato, S., and Cooper, D. M. (1994) Muscle energetics and pulmonary oxygen uptake kinetics during moderate exercise. *J. Appl. Physiol.* 77, 1742–1749
32. Wasserman, K., Stringer, W. W., Casaburi, R., and Zhang, Y. Y. (1997) Mechanism of the exercise hyperkalemia: an alternate hypothesis. *J. Appl. Physiol.* 83, 631– 643
33. Chuang, M. L., Ting, H., Otsuka, T., Sun, X. G., Chiu, F. Y., Beaver, W. L., Hansen, J. E., Lewis, D. A., and Wasserman, K. (1999) Aerobically generated CO(2) stored during early exercise. *J. Appl. Physiol.* 87, 1048 –1058
34. Stringer, W., Wasserman, K., Casaburi, R., Porszasz, J., Maehara, K., and French, W. (1994) Lactic acidosis as a facilitator of oxyhemoglobin dissociation during exercise. *J. Appl. Physiol.* 76, 1462– 1467
35. Walter, G., Vandenborne, K., Elliott, M., and Leigh, J. S. (1999) In vivo ATP synthesis rates in single human muscles during high intensity exercise. *J. Physiol. (London)* 519, 901–910
36. Kowalchuk, J. M., Smith, S. A., Weening, B. S., Marsh, G. D., and Paterson, D. H. (2000) Forearm muscle metabolism studied using (31)P-MRS during progressive exercise to fatigue after Acz administration. *J. Appl. Physiol.* 89, 200 –209

37. Gutmann, L. (2000) Periodic paralyses. *Neurol. Clin.* 18, 195–202
38. Ikeda, K., Iwasaki, Y., Kinoshita, M., Yabuki, D., Igarashi, O., Ichikawa, Y., and Satoyoshi, E. (2002) Acetazolamide-induced muscle weakness in hypokalemic periodic paralysis. *Intern. Med.* 41, 743–745
39. Ptacek, L. J. (1999) Ion channel diseases: episodic disorders of the nervous system. *Semin. Neurol.* 19, 363–369
40. Tawil, R., McDermott, M. P., Brown, R., Jr., Shapiro, B. C., Ptacek, L. J., McManis, P. G., Dalakas, M. C., Spector, S. A., Mendell, J. R., Hahn, A. F., et al. (2000) Randomized trials of dichlorphenamide in the periodic paralyses. Working Group on Periodic Paralysis. *Ann. Neurol.* 47, 46 –53
41. Fontaine, B., Vale-Santos, J., Jurkat-Rott, K., Reboul, J., Plassart, E., Rime, C. S., Elbaz, A., Heine, R., Guimaraes, J., and Weissenbach, J. (1994) Mapping of the hypokalaemic periodic paralysis (HypoPP) locus to chromosome 1q31–32 in three European families. *Nat. Genet.* 6, 267–272
42. Ptacek, L. J., Tawil, R., Griggs, R. C., Engel, A. G., Layzer, R. B., Kwiecinski, H., McManis, P. G., Santiago, L., Moore, M., and Fouad, G. (1994) Dihydropyridine receptor mutations cause hypokalemic periodic paralysis. *Cell* 77, 863– 868
43. Bulman, D. E., Scoggan, K. A., van Oene, M. D., Nicolle, M. W., Hahn, A. F., Tollar, L. L., and Ebers, G. C. (1999) A novel sodium channel mutation in a family with hypokalemic periodic paralysis. *Neurology* 53, 1932–1936
44. Jurkat-Rott, K., Mitrovic, N., Hang, C., Kouzmekine, A., Iaizzo, P., Herzog, J., Lerche, H., Nicole, S., Vale-Santos, J., Chauveau, D., et al. (2000) Voltage-sensor sodium channel mutations cause hypokalemic periodic paralysis type 2 by enhanced inactivation and reduced current. *Proc. Natl. Acad. Sci. USA* 97, 9549 –9554
45. Ptacek, L. J., Tyler, F., Trimmer, J. S., Agnew, W. S., and Leppert, M. (1991) Analysis in a large hyperkalemic periodic paralysis pedigree supports tight linkage to a sodium channel locus. *Am. J. Hum. Genet.* 49, 378 –382
46. Ptacek, L. J., Trimmer, J. S., Agnew, W. S., Roberts, J. W., Petajan, J. H., and Leppert, M. (1991) Paramyotonia congenita and hyperkalemic periodic paralysis map to the same sodium-channel gene locus. *Am. J. Hum. Genet.* 49, 851– 854
47. Rojas, C. V., Wang, J. Z., Schwartz, L. S., Hoffman, E. P., Powell, B. R., and Brown, R. H., Jr. (1991) A Met-to-Val mutation in the skeletal muscle Na+ channel alpha-subunit in hyperkalaemic periodic paralysis. *Nature (London)* 354, 387–389
48. Koch, M. C., Steinmeyer, K., Lorenz, C., Ricker, K., Wolf, F., Otto, M., Zoll, B., Lehmann-Horn, F., Grzeschik, K. H., and Jentsch, T. J. (1992) The skeletal muscle chloride channel in dominant and recessive human myotonia. *Science* 257, 797– 800
49. George, A. L., Jr., Crackower, M. A., Abdalla, J. A., Hudson, A. J., and Ebers, G. C. (1993) Molecular basis of Thomsen's disease (autosomal dominant myotonia congenita). *Nat. Genet.* 3, 305– 310
50. Plaster, N. M., Tawil, R., Tristani-Firouzi, M., Canun, S., Bendahhou, S., Tsunoda, A., Donaldson, M. R., Iannaccone, S. T., Brunt, E., Barohn, R., et al. (2001) Mutations in Kir2.1 cause the developmental and episodic electrical phenotypes of Andersen's syndrome. Cell 105, 511–519
51. Jurkat-Rott, K., and Lehmann-Horn, F. (2004) Periodic paralysis mutation MiRP2–R83H in controls: Interpretations and general recommendation. *Neurology* 62, 1012–1015
52. McCrossan, Z. A., Lewis, A., Panaghie, G., Jordan, P. N., Christini, D. J., Lerner, D. J., and Abbott, G. W. (2003) MinK- related peptide 2 modulates Kv2.1 and Kv3.1 potassium channels in mammalian brain. *J. Neurosci.* 23, 8077– 8091